

Examining the Length and Density Changes of Copper up to 300 °C under the Influence of Consciousness Bond Field: A Study of Taheri Consciousness Theory

Bahareh Kazazi^{1*}, Mohammad Ali Taheri²

1. Civil Engineering, CEO of Hoobe Construction Company, Tehran, Iran.

2. Sciencefact R&D Department, CosmoIntel Inc. Research Center, Ontario, Canada.

ABSTRACT

According to Taheri's theory of Consciousness, T-Consciousness can be converted into matter and energy and vice versa. Consciousness Bond Field is one of many Taheri Consciousness Fields (TCFs) founded and introduced by Mohammad Ali Taheri as new Fields. These Fields are neither matter nor energy; therefore, they do not possess a quantity, but they have direct effects on both matter and energy. In other words, although TCFs cannot be directly measured, we can investigate their effects indirectly through reproducible experiments. In this study, pure copper was selected to study its density and thermal behavior in the presence of the Consciousness Bond Field. Two meters of wire were cut from a cable and divided into two equal parts. Diffusion spectrometry was performed on the samples, and 15 pieces of 19.5 ± 0.25 mm were cut from each sample. The density of the samples was examined by the Archimedes method. The samples were then heated up to 300 °C. The relative increase in their lengths was examined at targeted temperatures, and the density of the samples was measured once more. Radiographic examination was performed on the 12 samples. The test results showed that all parts were healthy and free of defects. The changes in density followed a pattern opposite to those of the control samples and inconsistent with the known laws of material physics. Considering the increase in length, the density should have been decreased significantly compared to the control samples following dilatometry, but this was not the case. The density of the samples under the Consciousness Bond Field increased despite the increase gained in length. As the samples were undamaged and intact, the sample mass must have increased according to the concept of density and its increase. An XRD sample from each group was investigated. The observed changes gave the possibility of higher defects in the sample under TCF.

* Corresponding author:

Bahareh Kazazi
Civil Engineering, CEO of Hoobe Construction Company, Tehran, Iran.

Email: baharkazazi@gmail.com

Keywords: Consciousness Bond Field, Taheri Consciousness Fields, Copper Dilatometry, Densitometry

INTRODUCTION

Humans have always been curious to know the world around them. Many efforts have been made in this direction, which has led to the knowledge of various laws and fields such as gravitational field, electromagnetic field, electric field, etc. The term “field” has been used frequently in theories of physics.

The nature of consciousness and its place in science has received much attention in the current century. Many philosophical and scientific theories have been proposed in this area. In the 1980s, Mohammad Ali Taheri introduced novel fields with a non-material/non-energetic nature named Taheri Consciousness Fields (TCFs). In this perspective, T-Consciousness is one of the three existing elements of the universe apart from matter and energy. According to this theory, there are various TCFs with different functions, which are the subcategories of a networked universal internet called the Cosmic Consciousness Network (CCN). The major difference between the theory of TCFs and other theoretical concepts about consciousness is related to the practical application of the TCFs. TCFs can be applied to all living and non-living creatures, including plants, animals, microorganisms, materials, etc.

Mohammad Ali Taheri, the founder of Erfan Keyhani Halqeh, a school of thought, introduced a new science in 2020 as a branch of this school. He coined the term Sciencefact for this new science because it utilizes scientific investigations to prove the existence of T-Consciousness as an irrefutable phenomenon and a fact. Although science focuses solely on the study of matter and energy and Sciencefact, by contrast, explores the effects of the [non-material/non-energetic] TCFs, Sciencefact has provided a common ground between the two by conducting reproducible laboratory experiments

in various scientific fields, and it has used the scientific approach in proving TCFs.

The influence of the TCFs begins with the Connection between CCN as the Whole Taheri Consciousness of the universe and the subjects of study as a part. This Connection called “Ettesal” is established by the Announcer’s mind (a certified and trained individual who has been entrusted with the TCFs). The human mind has an intermediary role (Announcer) which plays a part by fleeting attention to the subject of study and then the main achievement obtained as a result of the effects of the TCFs. These Fields cannot be directly measured by science, but it is possible to investigate their effects on various subjects through reproducible laboratory experiments.

The research methodology in the study of T-Consciousness has been founded on the process of Assumption, Argument, and Proof, in which the Assumption is: The Cosmos was formed by a third element called T-Consciousness that is different from matter and energy.

The Argument is the existence of TCFs can be demonstrated by its effects on matter and energy (e.g., humans, animals, plants, microorganisms, cells, materials, etc.)

The Proof is the scientific verification of the effects of TCFs on matter and energy (according to the Argument) through various reproducible scientific experiments.

Accordingly, to investigate and verify the existence, effects, and mechanisms of TCFs, the following five research phases (Phases 0 through 4), and the aims of each phase are outlined below.

Phase-0 studies aim to prove the existence of TCFs by observing their effects. The nature of T-Consciousness and what it is will not be addressed in this phase. Phase-1 explores the varied effects of different TCFs. Phase-2 examines the reason behind the varied effects of these fields. Phase-3 investigates the mech-



Vol. 01
No. 07
April
2022

23

The First Journal in
T-Consciousness Research

anism of TCFs effects on matter and energy. Finally, Phase-4 draws significant conclusions, particularly with regard to the mind and memory of matter and their relation to the T-Consciousness, etc. [1, 2, 3].

Since any change in the structure and function of materials requires matter or energy, it is obvious that the study of the behavior of materials and their intrinsic, mechanical, and chemical properties in the presence of TCFs would be of value to scientific researchers. This research on the function and behavior of materials began over a decade ago and has yielded considerable results including the following.

Extensive research has also been conducted on cement mortar-based materials under the influence of TCFs. Although the purpose of previous research was to investigate the overall function, properties, and behavior of concrete and cement mortar, such as strength, concrete cancer, chloride diffusion coefficient, bending of concrete beams, penetration of gamma-neutron radiation, etc. under the influence of TCFs, in the present study, the process of internal changes revealed a number of details about how TCFs influence materials, including mass change during the application of TCFs [4-13].

In addition, different methods of nanomaterial synthesis, the study of tensile properties of metals, the study of angles of contact of water with a surface and change of silica mass in the thermal analysis due to the effects of TCFs without force or energy and matter, offer a revision of known laws and definitions of the behavior of the matter [1].

In the casting of pure 1000 series aluminum from a single ingot, after examining the crystal defects using two methods, it was found that the internal defects in some cases grew up to 1000%. In those samples, the only factor was the application of TCFs which had a significant effect on grid irregularities [3, 1]. Clearly, cre-

ating this level of displacement otherwise requires energy supply [4-13].

In the molecular software simulation of the behavior of aluminum, it was found that electron volts energy is created in the samples under the TCF if we consider the defects in half epsilon, assuming the mass remains constant per atom as (-3.10 eV) [13]. Given the background of the studies, the fundamental question was whether it is possible that underlying changes have taken place in the realm of the matter, and this is we have been overlooked due to the software limitations and the fact that mass has been kept constant?

Given these results, in the present research, pure copper was selected to investigate the thermal behavior and density changes before and after dilatometry up to 300 °C.

Materials and test methods

Preparation of the copper wire and analysis

It was unknown what effect the TCF would have on the matter. Also, the possibility of a change in volume, length, mass or distortion, etc., was given. This is because, in practice, the matter may not have the same expansion in all dimensions. For us, however, the basis for comparison was directly the measurement of volume. Therefore, considering any possible effects, the frequency, and the wire's diameter and length should have been measured at close intervals. This enabled us to measure the possible volume change over approximately two centimeters. However, such a test would have created a measurement error. In addition, the measurement alone was not effective due to the unknown mechanism of volume change under the TCF. Therefore, Archimedes' density was used as the initial measurement. This experiment was performed in three sets as follows:

Two meters of copper-filled solid wire with a diameter of 8 mm were cut. Emission spectrometry according to the BS EN 15079- 15 standard was performed. The wire was di-vided into two equal parts. One of the pieces was assigned to the Consciousness Bond Field test by the project executor and the other was assigned to the control by the laboratory official. Fifteen samples, each 19.5 ± 0.25 mm in length, were cut from each wire by the laboratory official. The density of each of the 9 samples was measured by the Archimedes method. All fifteen samples were then dilat-ed by the ASTM E289-17 standard up to 300 °C and after the changes, densitometry was performed again. To investigate the surface defects, industrial radiography before and after dilatometry was used for each group. A sample from each group was examined in order to evaluate the crystal changes. A 3mm piece was cut from one side. The two 3 mm pieces were then cut again (for 3mm) to bring the probe closer to the center of the pieces, and they were examined crystallographically (XRD).

Application of the Taheri Consciousness Field

One of the TCFs, called the Consciousness Bond Field, was applied to the samples according to the protocols regulated by the COSMOintel research center

(www.COSMOintel.com). A request for Connection to the CCN to utilize TCFs can be placed through the COSMOintel website in the "Assign Announcement" section. This access is available for everyone at no cost. In order to study and experience this Connection, the researchers can register on the website at any time in order to report the experiment to the COSMOintel research center. Certain details of the experiment must be provided to the center; for example, the characteristics or number and name of samples and controls must be specified. This entire experiment was carried out as a double-blind method where lab technicians were completely unaware of the TCFs theory, and the Announcer at the COSMOintel research center who established the Connection was unaware of the details of the study. Double-blind is a gold standard that is common in science experiments.

Results and discussion

Spectrochemical analysis

The result of the spectrochemical analysis test shows the percent abundance of possible elements in the sample and the purity level of the copper sample. It was determined from the results that the copper sample was 99.9% pure. The details are shown in Table 1.

Table 1 . The sample spectrometry

Zn	Pb	Sn	P	Mn
<0.01	0.01	<0.01	<0.005	Trace
S	Ag	Co	Be	Cu
None	Trace	0.01	<0.001	99.9
Fe	Ni	Si	Cr	Al
<0.005	0.03	<0.005	Trace	0.004



Increase in length

Following are the results of dilatometric analysis, as well as the relative increase in length

due to heat and the difference in density before and after dilatometry for the two groups (Table 2).

Table 2 . Increase in copper length due to heat and density changes

Name	100 °C	200 °C	300 °C		Before	After	
1	0.015	0.035	0.051	Density (±0.05) (g/cm ³)	8.84	8.83	-0.113
2	0.015	0.036	0.051		8.85	8.83	-0.225
3	0.016	0.034	0.051		8.85	8.84	-0.112
4	0.008	0.032	0.066		8.85	8.80	-0.564
5	0.009	0.034	0.067		8.81	8.81	0
6	0.008	0.032	0.066		8.82	8.79	-0.340
7	0.009	0.032	0.066		8.85	8.81	-0.451
8	0.008	0.036	0.068		8.86	8.81	0.564
9	0.006	0.032	0.063		8.85	8.80	-0.564
10	0.007	0.031	0.068				-0.488
11	0.007	0.032	0.065				
12	0.005	0.033	0.071				
13	0.006	0.031	0.06				
14	0.006	0.034	0.067				
15	0.006	0.032	0.067				
Average	0.008733	0.033067	0.063133				
fs1	0.016	0.037	0.055	Density (±0.05) (g/cm ³)	8.83	8.85	0.226
fs2	0.015	0.032	0.049		8.83	8.86	0.339
fs3	0.016	0.038	0.059		8.82	8.85	0.340
ck1	0.008	0.034	0.068		8.82	8.83	0.113
ck2	0.007	0.032	0.065		8.84	8.85	0.113
ck3	0.008	0.033	0.067		8.82	8.83	0.113
ck4	0.01	0.036	0.068		8.83	8.83	0
ck5	0.008	0.033	0.066		8.82	8.81	-0.113
ck6	0.009	0.034	0.069		8.82	8.82	0
c1	0.007	0.032	0.068				0.226
c2	0.008	0.035	0.07				
c3	0.007	0.031	0.066				
c4	0.006	0.034	0.067				
c5	0.005	0.035	0.071				
c6	0.006	0.033	0.065				
Average	0.009067	0.033933	0.064867				
%Change	3.80%	2.61%	2.74%				

To account for potential variability and minimizing possible errors, the experiment was repeated in three separate groups with multiple

samples. The results of the changes in each group were compared and examined with the average of the changes in the group, as shown in Table 3.

Table 3 . Comparison of average length changes in the tested groups increase in copper length due to heat and density changes

Series	100 °C	200 °C	300 °C
Control -Group1 average	0.015333	0.035000	0.051000
TCF-Group1 average	0.015667	0.035667	0.054333
Change %	2.70%	2%	6.50%
Control-Group2 average	0.008000	0.033000	0.066000
TCF-Group2 average	0.008333	0.033667	0.067167
Change%	4%	2%	1.70%
Control-Group3 average	0.006167	0.032167	0.066333
TCF-Group3 average	0.006500	0.033333	0.067833
Change%	5.30%	3.60%	2.30%

A laboratory official provided the numbers. According to the official protocol of the laboratory, the results are usually reported to the three decimal places. However, copper's longitudinal expansion coefficient is $17 \times 10^{-6} (1/k)$ and because of the very small length and the very low test temperature, the results

were reported with differences up to 6 decimal places. It was in order to be able to understand the length change properly.

In Table 4, the mean changes in the length of all samples under the influence of the Consciousness Bond Field are compared with the mean of the control samples.

Table 4 . Comparison of mean changes in the length of all the samples under the influence of Consciousness Bond Field compared to the control

All Controls Ave.	0.008733	0.033067	0.063133
All TCFs Ave.	0.009067	0.033933	0.064867
%Change	3.80%	2.61%	2.74%

According to the total results, the parts under the TCF seemingly had a relative increase in length compared with the control samples. This is because one factor that characterizes the behavior of materials under heat is the linear thermal expansion coefficient of the material presented by the laboratory.

Linear expansion coefficients

Linear expansion coefficients are the rate of

change of unit length per unit degree change in temperature. The coefficient of linear expansion of materials is found from the following formula:

$$\alpha = (dl/dT) * l / 1$$

Linear expansion coefficient is inversely related to the initial length of the sample and directly related to the length changes. In this study, the temperature was constant, and the results of linear expansion coefficients of samples are shown in Table 5 [14].

Table 5 . Linear expansion coefficients of the sample (All of the results are in 10⁻⁶ range)

Linear Thermal Expansion Coefficients 1/C° mm/mm			
Control		TCF	
Name	$\alpha \times 10^{-6}$	Name	$\alpha \times 10^{-6}$
1	18.2	fs1	18.8
2	18.2	fs2	17.4
3	17.8	fs3	19.0
Average	18.0	Average	18.4
4	15.6	ck1	15.6
5	14.8	ck2	15.5
6	16.6	ck3	15.1
7	13.8	ck4	15.6
8	15.6	ck5	16.8
9	15.6	ck6	15.1
Average	15.3	Average	15.6
10	14.9	c1	15.0
11	15.0	c2	14.6
12	14.6	c3	14.8
13	14.6	c4	14.5
14	15.1	c5	14.6
15	14.7	c6	15.1
Average	14.8	Average	14.9

Considering the linear expansion coefficients of pure copper that are $17 \times 10^{-6} (1/k)$, the length of samples tends to increase under the effect of the Consciousness Bond Field.

Obviously, given the length of the samples, the small temperature changes relative to the melting point of copper (1085 °C) [14], and only applying the TCF without any other external process, large changes are not expected. We will elaborate on the possibility of large changes later.

Comparison of density before and after dilatometry

This research is based on laboratory experiments on the possibility of changes in materials, on the other hand, any produced material, even if it is standard and high quality, has a few changes in the structure. Therefore, the best way to analyze the results is to compare the behavior of each piece before and after exposure to the Consciousness Bond Field. In order to do this, the density of each sample was compared before and after exposure. Figure 1 and Table 6 show the results.

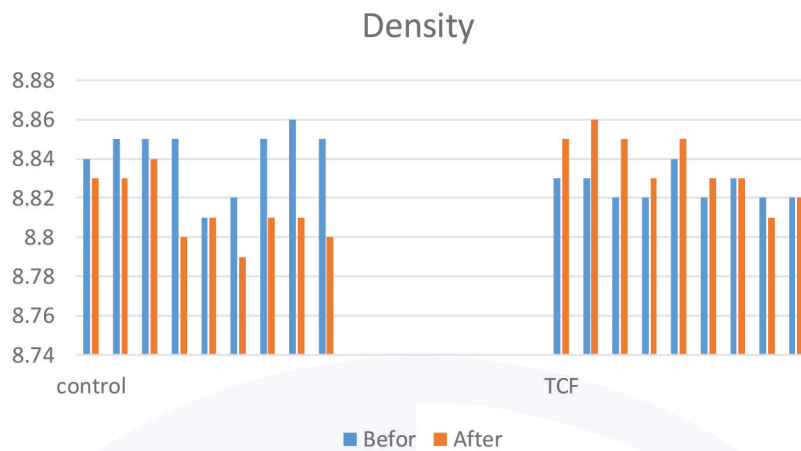


Figure 3. Comparison of changes in the density of samples

As results demonstrate, the samples under the Consciousness Field show an increase in the

density after the application of heat. The comparison of these changes is presented in Table 6.

Table 6 . The comparison of density changes in samples

Sample	300 °C Control			300 °C TCF			
	Before	After	Difference	Before	After	Difference	
1	8.84	8.83	-0.113	8.83	8.85	0.226	
2	8.85	8.83	-0.225	8.83	8.86	0.339	
3	8.85	8.84	-0.112	8.82	8.85	0.340	
4	8.85	8.80	-0.564	8.82	8.83	0.113	
5	8.81	8.81	0	8.84	8.85	0.113	
6	8.82	8.79	-0.340	8.82	8.83	0.113	
7	8.85	8.81	-0.451	8.83	8.83	0	
8	8.86	8.81	0.564	8.82	8.81	0.113	
9	8.85	8.80	-0.564	8.82	8.82	0	
Average	8.84	8.81	-0.488	8.83	8.84	0.226	
average difference of density%			-5.4%	average difference of density%			+2.5%
difference-in-difference of average density in two groups						7.9%	

Theoretical Discussion

The results of Table 2 show that the samples under the Consciousness Bond Field had an increase in the relative length. The linear thermal expansion coefficient of pure copper means that a unit of copper will have a relative increase of 0.000017 per unit of length. This coefficient depends on the magnitude of the temperature difference. Also, the melting temperature of copper is 1080 °C, which is 780 °C higher than the temperature of this experiment. As an example, the linear thermal expansion coefficient of cast Copper from ambient temperature to 100

°C from 17 to 18×10^{-6} [14].

These changes provide a better understanding of the effect of the T-consciousness Field which is non-material and non-energetic. It is very difficult to change the density of the crystalline solids. Copper has the atomic structure of FCC and is one of the most compact atomic lattices. In these atomic lattices, the copper atom contacts 12 other atoms, and 74% of the atomic lattice space is filled [16]. To better understand the required energy to change the density of copper, refer to an example where a copper sample with a length of 10 mm and

a cross-section radius of 2.4 mm with a cold-rolled coil equivalent to the strain of 4.5 with a magnitude of difference up to 4 decimal places had a density change of only 0.8% [16]. Therefore, any change in the structure of atomic lattices requires a considerable amount of energy.

Heating or cooling affects all the dimensions of a body of material, with a resultant change in volume. Volume changes may be determined from:

$$\Delta V/V_0 = \alpha V \Delta T$$

where ΔV and V_0 are the volume change and original volume, respectively, and αV represents the volume coefficient of thermal expansion. In many materials, the value of αV is anisotropic.

that is, it depends on the crystallographic direction along which it is measured. For materials in which the thermal expansion is isotropic, αV is approximately 3α [14].

Therefore, based on the principle of material and energy conservation and with the mass remaining constant, a 5.4% decrease in the average density difference was observed in the control group before and after dilatometry. On the contrary, the density has increased in the samples under the Consciousness Field. This is despite the fact that the average density of these samples before dilatometry was

0.01 (g/cm³) less than the control samples. A 1.5% higher linear expansion coefficient leads to a 4.5% higher volumetric thermal expansion coefficient. Therefore, the volume of the samples under the TCF has theoretically become much larger. If the mass remained constant, theoretically, the density of the samples under the TCF after dilatometric should have had a much smaller density than the control sample ($\rho = m/V$). The difference in differences in the density of the samples compared with the control group was (-5.4%) + (2.505) = 7.9% which is a much higher density. This change is only possible by creating a heavier mass. However, for both groups, part of the increase in volume has returned to normal after cooling.

In this study, there is one sample with high dispersion in each group, and if only numerical and theoretical studies were considered, these samples would have been removed and the difference would have been much larger. But our basis in this study is only experimental data and no observation was excluded. According to Taheri's theory of T-Consciousness, the third factor, which is neither energy nor matter but can be converted into matter and energy, is T-Consciousness. Despite the compactness of the copper atomic lattice, how T-Consciousness has made matter denser and what changes have taken place in the copper atomic lattice needs more research.

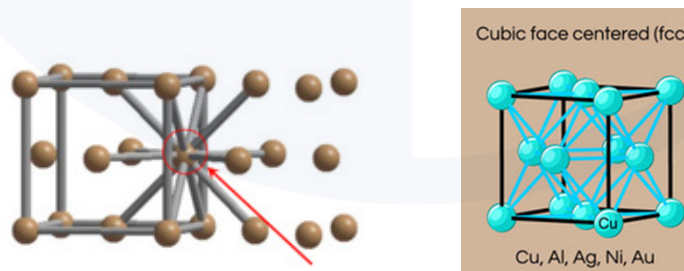


Figure 2. Schematic picture of the copper crystal lattice

Radiographic results

Among the factors checked for accuracy was the accuracy of the parts before and after dilatometry. A check was made to ensure that they

were free of cracks and holes. For this reason, radio-graphs were taken of the second series. The original radiographic reports are provided in the following in figures 3 and 4.

Revision number : 0		Radiographic test report							Reference code/standard : —			
Nominal Thickness (mm)	No. of film	Film Size (cm)	Visible IQI	Repair	Reject	Accept	Order No.	Segment	Type of defect(s) / location / Dimension			
---	1	10*20	Wire 12	---		*	38157 1-6	B-CK 1-6	Not Seen			
Source Type	Source size (mm*mm)	Total film length(cm)	IQI Type	Film type	Screen Type	Exposure Technique	Ug (mm)	Sensitivity %	Density	SFD (cm)	Exposure Time (minute)	Source Strength(Kv)
X-RAY	2*2	20	10-16 Cu	Kodak AA400	Lead	SWSI	≤ 0.51	1-2	1.8-4	60	0.4	170
Abbreviation	Type of Weld Defects				Technique				Other			
	LOP: Lack of Penetration				SWSI: Single Wall Single Image				SFD: Source To Film Distance			
	LOF: Lack of Fusion				DWSI: Double Wall Single Image				IQI: Image Quality Indicator			
	TI: Tungsten Inclusion				DWDI: Double Wall Double Image				No.: Number			
*REMARK: Test result shall be considered by the customer.												

Revision number : 0		Radiographic test report							Reference code/standard : —			
Nominal Thickness (mm)	No. of film	Film Size (cm)	Visible IQI	Repair	Reject	Accept	Order No.	Segment	Type of defect(s) / location / Dimension			
---	1	10*20	Wire 12	---		*	38157 1-6	A-CK 1-6	Not Seen			
Source Type	Source size (mm*mm)	Total film length(cm)	IQI Type	Film type	Screen Type	Exposure Technique	Ug (mm)	Sensitivity %	Density	SFD (cm)	Exposure Time (minute)	Source Strength(Kv)
X-RAY	2*2	20	10-16 Cu	Kodak AA400	Lead	SWSI	≤ 0.51	1-2	1.8-4	60	0.4	170
Abbreviation	Type of Weld Defects				Technique				Other			
	LOP: Lack of Penetration				SWSI: Single Wall Single Image				SFD: Source To Film Distance			
	LOF: Lack of Fusion				DWSI: Double Wall Single Image				IQI: Image Quality Indicator			
	TI: Tungsten Inclusion				DWDI: Double Wall Double Image				No.: Number			
*REMARK: Test result shall be considered by the customer.												

Figure 3. Radiography before and after dilatometry of ck samples under the T-Consciousness Field

Revision number : 0		Radiographic test report							Reference code/standard : —			
Nominal Thickness (mm)	No. of film	Film Size (cm)	Visible IQI	Repair	Reject	Accept	Order No.	Segment	Type of defect(s) / location / Dimension			
---	1	10*20	Wire 12	---		*	38157 7-12	B-1-6	Not Seen			
Source Type	Source size (mm*mm)	Total film length(cm)	IQI Type	Film type	Screen Type	Exposure Technique	Ug (mm)	Sensitivity %	Density	SFD (cm)	Exposure Time (minute)	Source Strength(Kv)
X-RAY	2*2	20	10-16 Cu	Kodak AA400	Lead	SWSI	≤ 0.51	1-2	1.8-4	60	0.4	170
Abbreviation	Type of Weld Defects				Technique				Other			
	LOP: Lack of Penetration				SWSI: Single Wall Single Image				SFD: Source To Film Distance			
	LOF: Lack of Fusion				DWSI: Double Wall Single Image				IQI: Image Quality Indicator			
	TI: Tungsten Inclusion				DWDI: Double Wall Double Image				No.: Number			
*REMARK: Test result shall be considered by the customer.												

Revision number : 0		Radiographic test report							Reference code/standard : —			
Nominal Thickness (mm)	No. of film	Film Size (cm)	Visible IQI	Repair	Reject	Accept	Order No.	Segment	Type of defect(s) / location / Dimension			
---	1	10*20	Wire 12	---		*	38157 7-12	A-1-6	Not Seen			
Source Type	Source size (mm*mm)	Total film length(cm)	IQI Type	Film type	Screen Type	Exposure Technique	Ug (mm)	Sensitivity %	Density	SFD (cm)	Exposure Time (minute)	Source Strength(Kv)
X-RAY	2*2	20	10-16 Cu	Kodak AA400	Lead	SWSI	≤ 0.51	1-2	1.8-4	60	0.4	170
Abbreviation	Type of Weld Defects				Technique				Other			
	LOP: Lack of Penetration				SWSI: Single Wall Single Image				SFD: Source To Film Distance			
	LOF: Lack of Fusion				DWSI: Double Wall Single Image				IQI: Image Quality Indicator			
	TI: Tungsten Inclusion				DWDI: Double Wall Double Image				No.: Number			

Figure 4. Radiography before and after dilatometry of the control samples



The test results showed that all parts were healthy and free of defects. Density numbers and length changes depended on the healthy

part and were not because of the cavities or cracks. The radiographic images of the samples are provided here.

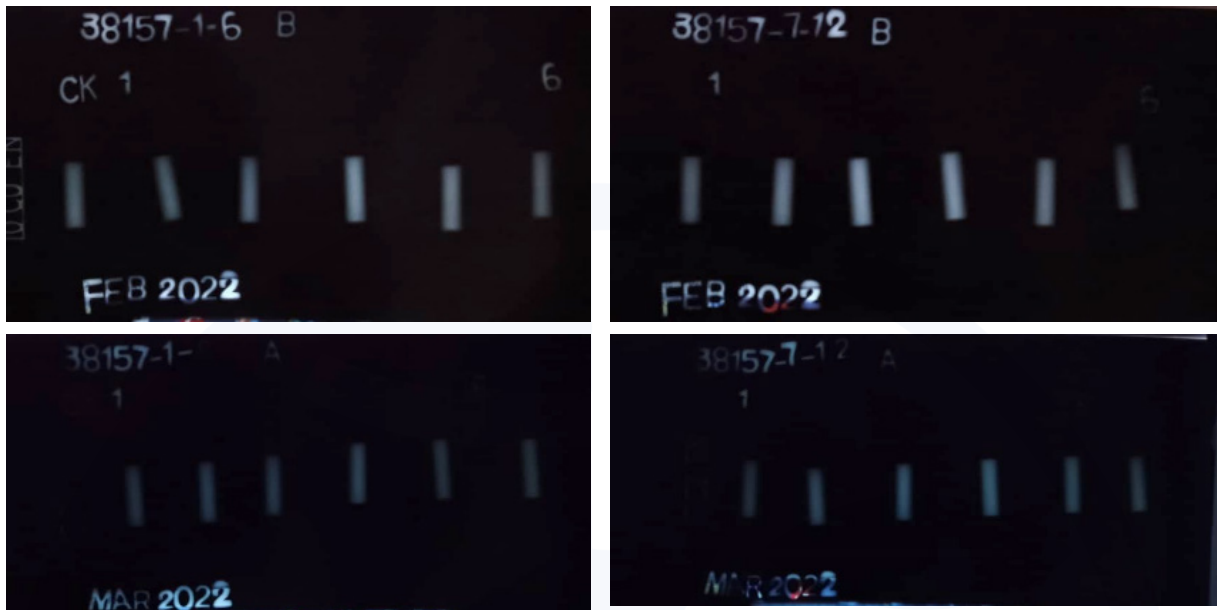


Figure 5. Radiography of the samples. The images on the right are the control samples, and the images on the left are the samples under the influence of the Consciousness Bond Field. The images on the top are before dilatometry and the images on the bottom are after dilatometry.

XRD (X-Ray Diffraction Crystallography)

XRD test was used to evaluate the changes in the crystal structure of the two experimental

samples. The X-ray diffraction patterns of these two samples are shown in Figure 6. Tests were performed with a copper anode at a voltage of 30 mA and a current of 40 kV. Step size was 0.05° and counting time per step was 0.5 sec.

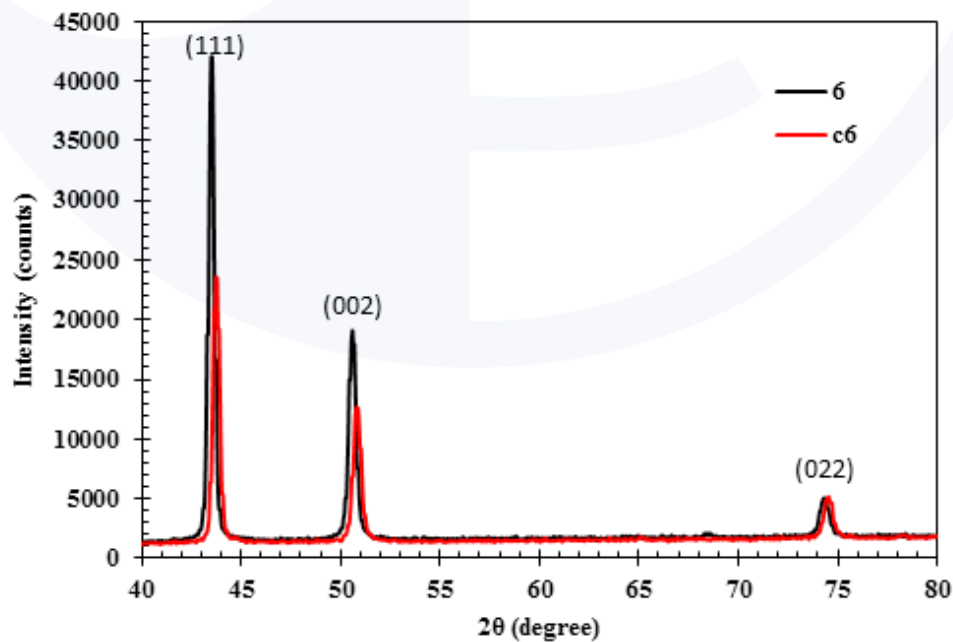


Figure 6. The X-ray diffraction pattern of the experimental samples [C6:TCF & 6: Control]

X'Pert Highscore Plus software was used to identify the phase from the results of the X-ray diffraction pattern of these samples. According to Figure 6, it is clear that in these samples only one crystalline phase is formed. By adapting these peaks to the reference diffraction patterns by the mentioned software, it was found that these two samples had the highest compliance with the copper structure with the reference code JCPDS No. 968-431-3208 has a cubic crystal structure and Fm-3m space group (FCC structure). The diffraction plates of each peak are shown on the same peak in Figure 6. According to Figure 6, two major changes in diffraction patterns are observed for these two samples. The first change is related to the higher diffraction intensity of some peaks in sample 6 than in sample c6 and the second change is the displacement of peaks related to sample c6 to the higher angles. In general, the increase in the intensity of crystalline peaks can be attributed to the increase in the degree of crystallinity of the structure [17]. Therefore, the lower crystallinity of sample c6 may be due to the presence of crystal defects in the structure of this material. On the other hand, displacement of the peaks can be attributed to the distance between the plates and the lattice parameter according to Bragg law [18].

$$(1) \quad (n\lambda = 2d\sin\theta)$$

Where n is a constant value (here equal to 1), λ is the X-ray wavelength (here 1.54 angstroms), d is the spacing of the diffraction between the graphene oxide plates and θ is the location of the peak. Accordingly, the distance between the crystal plates decreases with the increasing angle of the peak. Thus, the distance between the diffraction plates (111), (002), and (022) decreased from 2,091, 1,811, and 1,281 angstroms in sample 6 to

2,090, 1,810 and 1,280 angstroms in sample c6, respectively. On the other hand, the value of the distance between the plates according to Equation 2 in the cubic crystal lattice is related to the lattice parameter (the distance between two atoms in the crystal lattice) [19].

$$(2) \quad d = a / (h^2 + k^2 + l^2)^{0.5}$$

Where d is the distance between the crystal plates, a is the lattice parameter, and h, k, and l are the Miller indices of the diffraction plates. Accordingly, and due to the fact that the Miller indices are constant for the two samples, the reduction of the plate spacing in sample c6 compared to sample 6 can be attributed to the lower lattice parameter in this sample than in sample 6. According to this relation, the lattice parameters for samples c6 and 6 are equal to 3.622 and 3.620 angstroms, respectively. This lower lattice parameter may be due to defects such as gaps in the c6 crystal structure.

The size of the crystal and the macrostrain related to the structure of the two materials can also be calculated from the results of the XRD test. To calculate these parameters, the MAUD Rietveld software was used. It is a technique introduced by Hugo Rietveld for identification of the crystalline materials. In this technique, the height, width, and position of each peak in its X-ray diffraction pattern can be used to determine many structural aspects of the material. Rietveld's technique uses the least-squares method to better fit the theoretical values on the measured values [20,21]. According to the results of this method, the crystal size of samples 6 and c6 are 100.5 and 95.4 nm, respectively. Also, the microstrain of the structure of these two samples are equal to 0.0020 and 0.0022, respectively. The higher microstrain of the c6 structure can be considered another reason for the lattice distortion due to the structural defects.

Conclusion

In this study, 99.9% pure copper was used. According to the results of the dilatometric test, the samples under the influence of the Consciousness Bond Field had a significant increase in length. Therefore, the first result was a change in length of pure copper up to 300 °C in the presence of the Consciousness Bond Field compared to the control sample. Also, the samples whose density was measured before and after dilatometry showed a pattern of density change opposite to that of the control samples. Due to the increase in length, it is obvious that the sample volume has increased and according to the definition of density, the density should have decreased after dilatometry, which was the case in the control samples. But in the samples under the influence of the Consciousness Bond Field, the density increased. This is related to the increase in the mass of samples under the influence of the Consciousness Bond Field.

Moreover, radiographs of the samples showed that an increase in the length did not cause destruction in the samples and the samples were all intact. And the increase in length and changes in density were not a result of changes in appearance or defects in the samples. Given that the experimental conditions were constant and that the only variable was

the presence of the Consciousness Bond Field, we can attribute the results to Taheri's theory of T-Consciousness which states T-Consciousness can be converted to both matter and energy, and so the increased density. According to the XRD results, the crystal size of samples 6 and c6 are 100.5 and 95.4 nm, respectively. Also, the microstrain of the structure of these two samples are equal to 0.0020 and 0.0022, respectively. The higher microstrain of the c6 structure can be considered another reason for the lattice distortion due to the structural defects.

One of the possible reasons for the increase in mass could be the effect on the crystal lattice distortion. Considering the compact atomic lattices of copper, any further compaction would lead to higher defects.

Due to the novelty of this idea and its comprehensiveness, it is recommended to examine the possibility of changes in the atomic structure and crystal lattices of other materials as well as subatomic changes and theories for denser particles. The investigation will enable us to further findings on the effects of the Consciousness Bond Field on the matter.

Acknowledgment

We appreciate the sincere cooperation of the Razi Metallurgy Research Center.

References

1. Taheri, M. A. (2020). The main monitoring center for T-Consciousness Fields research and studies based on Sciencefact. www.Cosmointel.com.
2. Taheri, M. A. (2012). General Connection of Particles. Interuniversal Publishing Erfan-Halgheh. ID: 978-1-940491-03-5.
3. Taheri, M. A. (2013). Human from Another Outlook (2nd Edition). ISBN-I3: 978-1939507006, ISBN- 10: 1939507006.
4. Kazazi, B, & Taheri, M. A. (2021). Effect of the Consciousness Bond Field on the structure and properties of Aluminum. Retrieved from www.cosmointel.com.
5. Kazazi, B, & Taheri, M. A. (2021). Effect of the Consciousness Bond Field on the structure and properties of 1000- series Aluminum-with preheating Retrieved from www.cosmointel.com.
6. Kazazi, B, & Taheri, M. A. (2021). Study of density changes and increase in the length of pure copper up to 300 °C in Consciousness Bond Field. Retrieved from www.cosmointel.com.
7. Kazazi, B, & Taheri, M. A. (2021). Study of the effect of the Consciousness Bond Field on mechanical crushing of silica particles preheating Retrieved from www.cosmointel.com.
8. Kazazi, B, & Taheri, M. A. (2021). Influence of Consciousness Bond Field on the plant synthesis of nano-silver preheating Retrieved from www.cosmointel.com.
9. Kazazi, B., & Taheri, M. A. (2021). Influence of Consciousness Bond Field (CF) on crystallization and strength of cement mortar (concrete). Retrieved from www.cosmointel.com.
10. Kazazi, B., & Taheri, M. A. (forthcoming 2022). Comparison of the behavior of concrete made under the influence of Taheri Consciousness Fields (TCFs), and under gamma and neutron radiations, with ordinary concrete, when receiving TCF and gamma and neutron radiations simultaneously.
11. Kazazi, B., & Taheri, M. A. (forthcoming 2022). Investigation of chlorine ion penetration in concrete under the influence of Taheri Consciousness Fields.
12. Kazazi, B., & Taheri, M. A. (2021). Effects of the T-Consciousness Field on Concrete (ASR. Retrieved from www.cosmointel.com.
13. Kazazi, B, & Taheri, M. A. (forthcoming 2022). Molecular software simulation of the behavior of aluminum under TCFs.
14. ASM International. www.asminternational.org
15. WWW.nano.ir
16. Forouzanmehr N, Nili-Ahmadabadi M, Abdous H, Fallahi B.(2020). On the free volumes of severely deformed pure Fe and Cu, similarities and differences. Metallurgical Engineering, 23(1): 4-15 <http://dx.doi.org/10.22076/me.2020.112690.1255>
17. Inoue M, Hirasawa I. (2013). The relationship between crystal morphology and XRD peak intensity on CaSO₄·2H₂O. Journal of Crystal Growth; 380:169–75. doi:10.1016/J.JCRYSGRO.2013.06.017.
18. Fish PW. (1971). Electron diffraction and the Bragg equation. Physics Education;6:002. doi:10.1088/0031-9120/6/1/002.
19. Mousa AM, Haider AJ, Al-jawad SMH. (2011). Optical Properties of Nanostructure in CdS at Different Condition Bath Optical Properties of Nanostructure in CdS at Different Condition Bath Deposition. Journal of Materials Science and Engineering ;5:184–91. doi:10.17265/2161-6213/2011.02.011.
20. Hernandez CC, Ferreira FF, Rosa DS. (2018). X-ray powder diffraction and other analyses of cellulose nanocrystals obtained from corn straw by chemical treatments. Carbohydrate Polymers;193:39–44. doi:10.1016/j.carbpol.2018.03.085.
21. Ju X, Bowden M, Brown EE, Zhang X. (2015). An improved X-ray diffraction method for cellulose crystallinity measurement. Carbohydrate Polymers;123:476–81. doi:10.1016/j.carbpol.2014.12.071.



Vol. 01
No. 07
April
2022

35

The First Journal in
T-Consciousness Research